A High-Speed Photonic Clock and Carrier Regenerator

X. S. Yao and G. Lutes
Communications Systems Research Section

As data communications rates climb toward 10 Gbits/s, clock recovery and synchronization become more difficult, if not impossible, using conventional electronic circuits. The high-speed photonic clock regenerator described in this article may be more suitable for such use. This photonic regenerator is based on a previously reported photonic oscillator capable of fast acquisition and synchronization. With both electrical and optical clock inputs and outputs, the device is easily interfaced with fiber-optic systems. The recovered electrical clock can be used locally and the optical clock can be used anywhere within a several kilometer radius of the clock/carrier regenerator.

I. Introduction

In high-speed fiber-optic communications systems, the ability to recover the clock from the incoming random data is essential. The recovered clock must be in precise synchronism with the incoming data and is used in further signal processing systems, such as regenerative repeaters, time division switching systems, and demultiplexers.

Conventional clock recovery devices are generally based on electronic phase-locked loops (PLLs) [1]. These devices may not be suited for the high-speed fiber-optic communications system because of their relatively slow speed, slow acquisition time, narrow tracking range, inability to be tuned over a wide range of frequencies, and non-optical inputs and outputs. Having optical inputs and outputs is important because it makes interfacing with a fiber-optic system easier.

All optical clock recovery schemes proposed by many authors [2–6] are based on injection locking a pulsed laser with the incoming data stream, wherein the pulsed laser has a nominal pulsation rate close to the incoming data rate. In one scheme, the pulsed laser [2–4] is a mode-locked fiber ring laser, and the input data modulates the laser cavity length or loss via the optical nonlinear effect. Because optical nonlinearity is used, the intensity of the injection data has to be high and is, therefore, not practical in many applications. In another scheme, the pulsed laser is a self-pulsating semiconductor laser [5,6] where the self-pulsation is caused by self-Q-switching within the device. The pulsation rate can be controlled by varying the current to the device. The problems associated with such a device are the relatively low speed (a few GHz) and relatively high noise.

Although the concept of all optical systems is attractive, the majority of present and future systems will be hybrid, meaning that the system can be controlled and accessed both optically and electronically.

Appendix

Performance of Two Cascaded Phase-Locked Loops

The analysis of cascaded loops was considered in the past by several authors [14–16] for the purpose of determining accurate two-way Doppler and phase measurements between an antenna and a spacecraft in order to determine the relative position and velocity of the spacecraft. Here, in the carrier-aiding scheme, we are interested in determining accurately the loop SNR of the aided loop and the joint pdf of the two carrier phase error processes. Therefore, to accomplish that, we can apply the results of [14], keeping in mind that, in our case, the two cascaded loops are both in the downlink.

The proposed solution in [15], which is based on Fokker–Planck techniques and verified by simulation, takes on the following form:

$$p(x_1, x_2) = \frac{\exp\{a_2 \cos[(x_2 - m_2) - a(x_1 - m_1)] + a_1 \cos(x_1 - m_1)\}}{(2\pi)^2 I_0(a_2) I_0(a_1)} \tag{A-1}$$

where

$$\left.\begin{aligned} a_1 &= \frac{1}{\sigma_1^2} \\ a_2 &= [\sigma_2^2(1-\rho^2)]^{-1} \\ a &= \frac{\eta\sigma_2}{\sigma_1} \end{aligned}\right\} \tag{A-2}$$

within the region

$$-\pi \le x_i \le \pi \text{ for } i = 1, 2$$

and

$$(x_1, x_2) = \begin{cases} (\hat{\theta}_1, \hat{\theta}_2) & \text{then } (m_1, m_2) = (\theta_1, \theta_2 + \hat{\theta}_1) \\ (\hat{\phi}_1, \hat{\phi}_2) & \text{then } (m_1, m_2) = (0, 0) \end{cases}$$

The σ_1^2, σ_2^2, ρ, m_1, and m_2 are the parameters of the two-dimensional Gaussian density to which either $p(\hat{\theta}_1, \hat{\theta}_2)$ or $p(\hat{\phi}_1, \hat{\phi}_2)$ converge at high SNR, which must be determined in terms of the cascaded loop system parameters in order to characterize the joint density function as given in Eq. (A-1). The results that are stated here are specialized to second-order loops with imperfect integrators and damping parameters equal to 2.

Therefore, a clock recovery device having such a hybrid capability is important, and in this article we report such a device—the photonic clock regenerator. We also show that the same device can be used for high-frequency carrier recovery and will be useful in fiber-optic analog communications systems.

The photonic clock and carrier regenerator is based on the photonic oscillator described in an earlier article [7]. As shown in Fig. 1, functionally it is a six-port device with an optical and an electrical injection port, an optical and an electrical output port, and two voltage-controlling ports for tuning frequency. The incoming data are injected into the photonic oscillator either optically or electrically. The free-running photonic oscillator is tuned to oscillate at a nominal frequency close to the clock frequency of the incoming data. With the injection of the data, the photonic oscillator will be quickly phase locked to the clock frequency of the data stream while rejecting other frequency components (harmonics and subharmonics) associated with the data. Consequently, the output of the locked photonic oscillator is a continuous periodic wave synchronized with the incoming data, or simply the recovered clock.

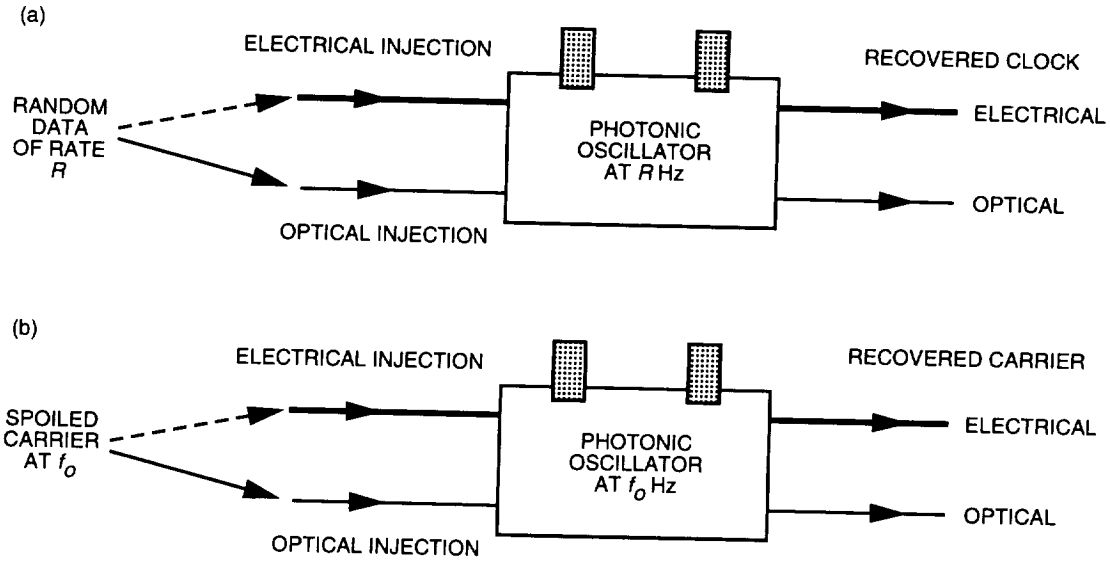

Fig. 1. Functions of the photonic clock and carrier regenerator: (a) clock recovery and (b) carrier recovery.

II. Clock Recovery Demonstration

Figure 2 shows the clock recovery experiment setup. An HP 8080 Word Generator System was used to generate a stream of repetitive 64-bit words at 100 Mbits/s, and the photonic oscillator was tuned to oscillate at 100 MHz. The data were injected into the bias port of the electro-optical (E/O) modulator through a filter and a bias T. The filter was centered at 100 MHz with a 3-dB bandwidth of 10 MHz. It was used to reduce unwanted frequency components of the input data. The output of the photonic oscillator was fed either into a spectrum analyzer (HP 8562) or an oscilloscope (Tektronix 2465B). When using the oscilloscope, the first bit of each word was used to trigger the sweep so the whole word could be displayed.

Note that although a photonic clock regenerator is capable of recovering a clock at much higher frequencies (up to 70 GHz), due to equipment constraints we chose to demonstrate clock recovery at 100 MHz to make our measurements easier. With the HP 8080 system, the data pattern can easily be selected to be either return-to-zero (RZ) or non-return-to-zero (NRZ), so both types of data were tested in our experiments. The selected 64-bit word was 0010101101101001 0110001110101101 1011001010001010 0010101100101000. The clock recovery is independent of the word chosen, as long as it is balanced.

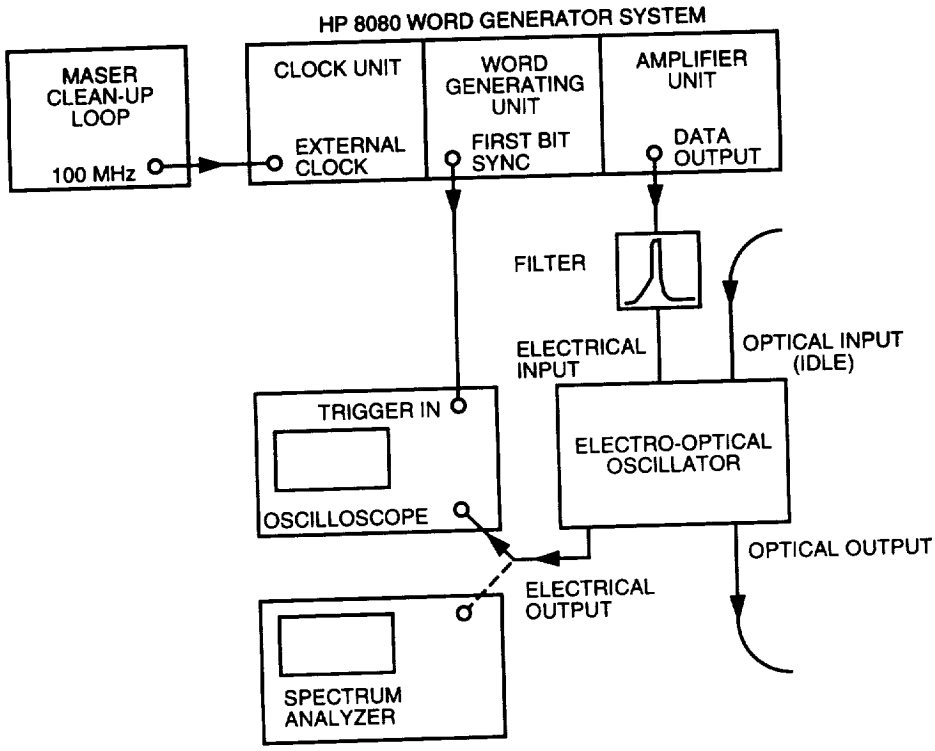

Fig. 2. Clock recovery experiment setup.

Figure 3 shows the experiment results in the frequency domain that demonstrated successful clock recovery from an NRZ data stream. The frequency spectrum of the input data is measured with the 100-MHz filter and is identical to the injected signal. As one can see, the selected NRZ data stream has some frequency components stronger than the clock frequency. After clock regeneration, the recovered clock is 62-dB stronger than the strongest harmonic component. Figure 4 shows the same experiment results in the time domain. Figure 4(a) shows the traces of the input data (lower trace) and the trigger signal (upper trace). Figure 5 contains the same information as Fig. 4, except that the time span is reduced 10 times so that the details of the traces can be seen. It is evident that the recovered clock is a perfect sine wave. The fact that the recovered clock can be clearly displayed on the oscilloscope when the first bit of data is used as the trigger indicates that the recovered clock is synchronized with the data. If the photonic oscillator is not locked to the data (free running), its phase wanders relative to the data bits. As a result, the display of the photonic oscillator's output signal on the oscilloscope is smeared when any data bit is used to trigger the oscilloscope, as shown in Fig. 6. Note the recovered clock level is almost independent of the input signal level, a feature that is desirable for clock recovery and is inherent in injection-locked oscillators. Other proposed high-speed clock recovery circuits use automatic gain control and limiting amplifiers to achieve constant amplitude [8].

We have also successfully demonstrated photonic clock recovery from RZ formatted data. Because the RZ data have a higher level of the clock frequency component, recovering the clock is more straightforward than recovering the clock from NRZ data. Similar results are expected for optical injection since the data in the optical domain will be automatically converted by the internal photodetector into the electrical domain before affecting the photonic oscillator. Note that for infinitely long NRZ random data, the clock frequency component is zero. In order to recover the clock from such a data stream, a procedure to convert NRZ data format to RZ format is required [1].

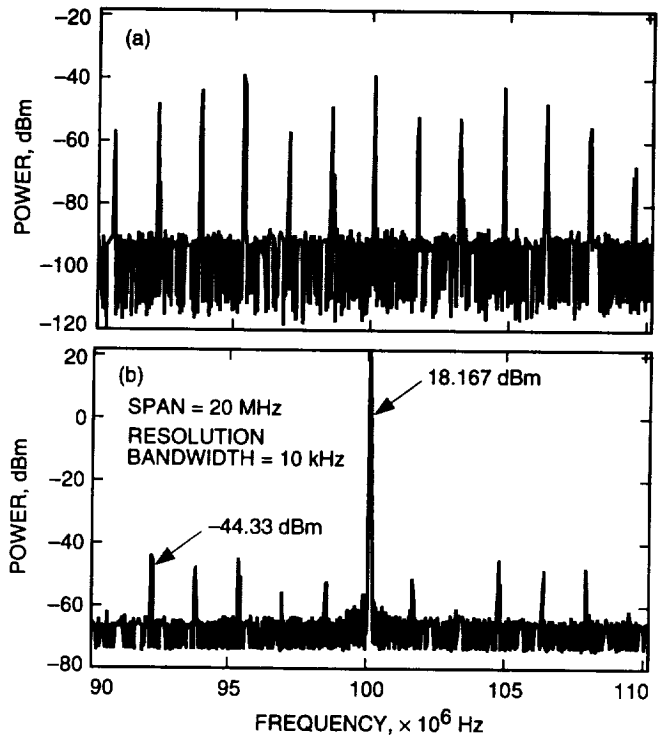

Fig. 3. Clock recovery from an NRZ data stream measured in the frequency domain: (a) random data input and (b) recovered clock.

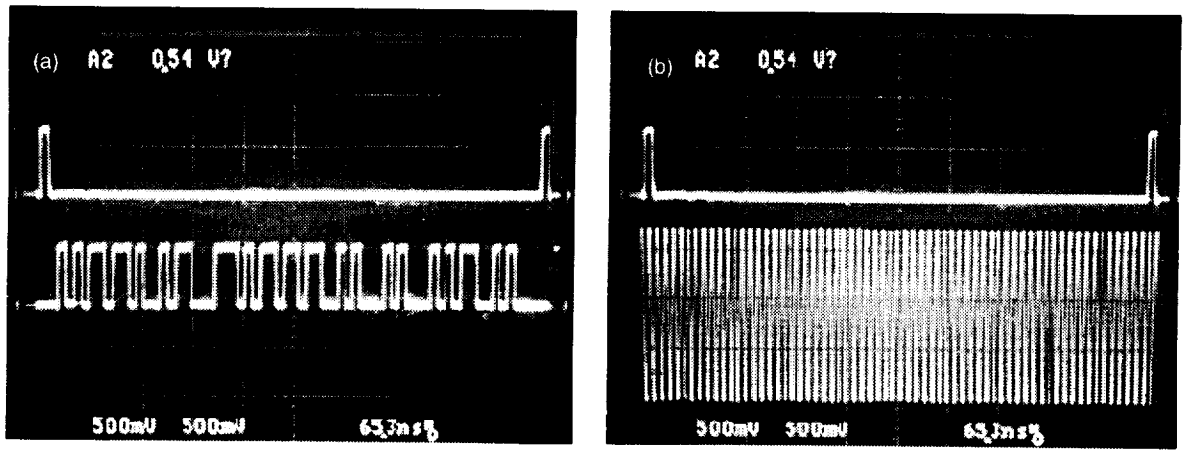

Fig. 4. Clock recovery from an NRZ data stream measured in the time domain: (a) random data input and (b) recovered clock.

III. Carrier Recovery Demonstration

Similar to clock recovery, a carrier buried in noise can also be recovered by the photonic oscillator. To do so, we simply inject the spoiled carrier into the photonic oscillator that has a free-running frequency close to the carrier frequency and an output power level $N(N >> 1)$ dB higher than the carrier level. The injected carrier forces the photonic oscillator to be locked with the carrier and results in an equivalent carrier gain of N dB. Because the open-loop gain of the photonic oscillator is only n dB ($n \approx 1$), the noise of the input is amplified by only n dB and the signal-to-noise ratio of the carrier is then increased by $(N - n)$ dB.

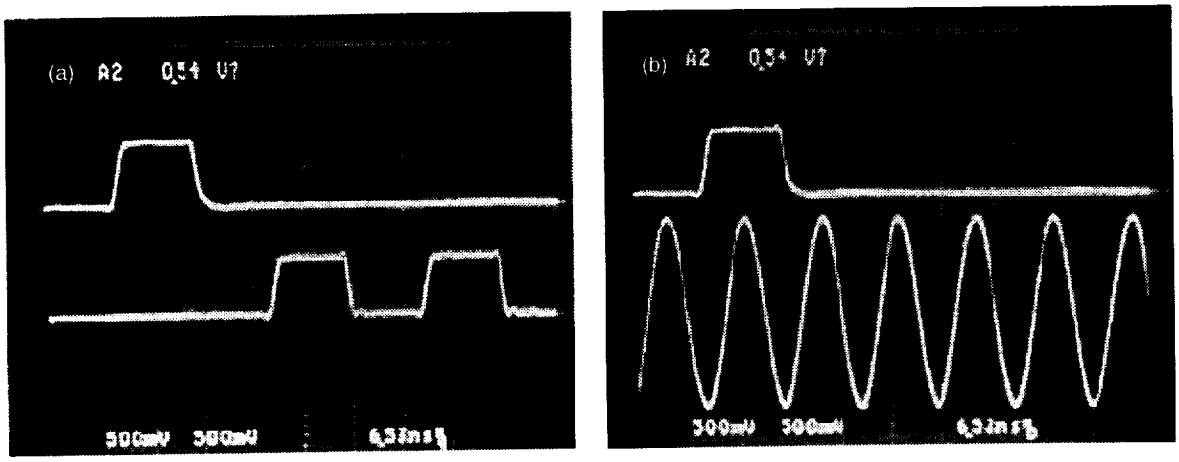

Fig. 5. The data trace of Fig. 4, with the time span reduced 10 times: (a) random data input and (b) recovered clock.

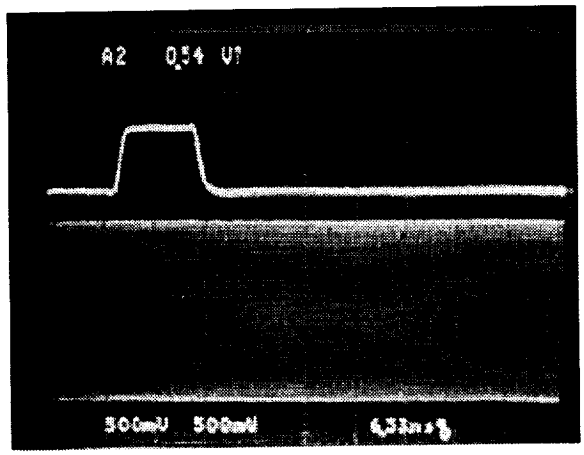

Fig. 6. The data trace where the photonic oscillator is not locked to the data.

Figure 7 is the experiment setup for demonstrating the photonic carrier recovery. In the experiment, a clean 100-MHz carrier from an H-maser frequency standard and a clean-up loop is combined with a noise source consisting of two noisy amplifiers in series. The resulting spoiled carrier was measured using the spectrum analyzer and is shown in Fig. 8(a). Figure 8(b) shows the spectrum of the recovered carrier, and it is evident from the figure that the signal-to-noise ratio of the carrier is increased by more than 50 dB. We also measured the spoiled carrier and recovered carrier in the time domain with an oscilloscope, and the results are shown in Fig. 9. In both Fig. 9(a) and Fig. 9(b), the upper trace (a square pulse) is the trigger signal and the lower trace is the carrier. Comparison of the two figures clearly demonstrates the effectiveness of the photonic oscillator as a carrier recovery device.

IV. Attractive Properties of the Photonic Clock and Carrier Regenerator

Our experiment results and analysis indicate that the photonic clock and carrier regenerator described above has the following attractive properties:

(1) High-speed or high-frequency operation. The speed of the device can be as high as 70 GHz and is limited only by the speed of the photodetector and the E/O modulator used. We have demonstrated a photonic oscillator operating as high as 9.2 GHz.

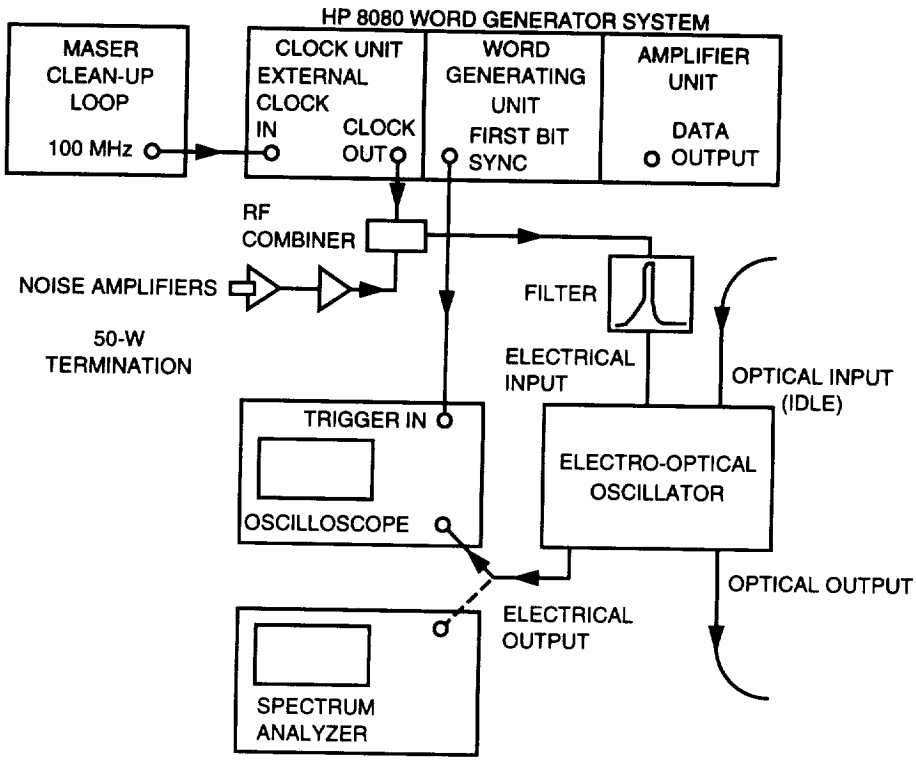

Fig. 7. Experiment setup for demonstrating photonic carrier recovery.

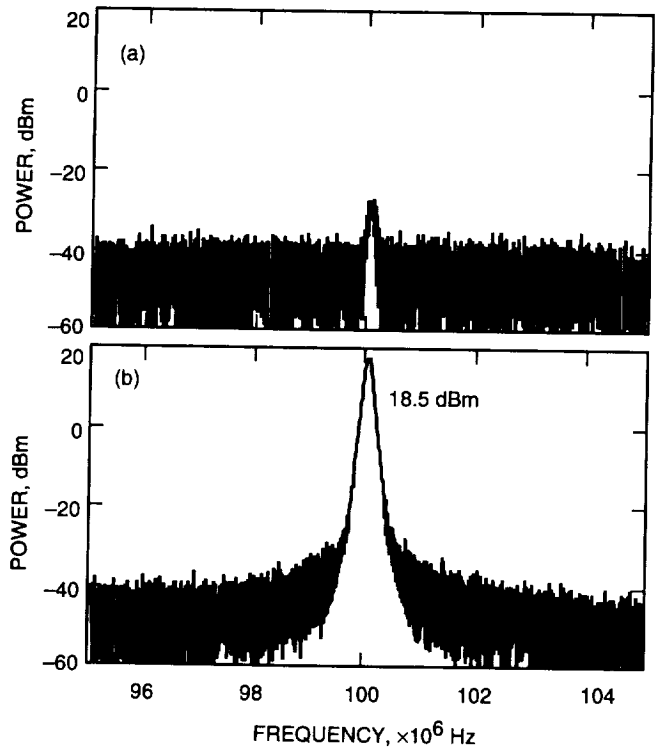

Fig. 8. Carrier recovery measurement in the frequency domain: (a) spoiled carrier and (b) recovered carrier.

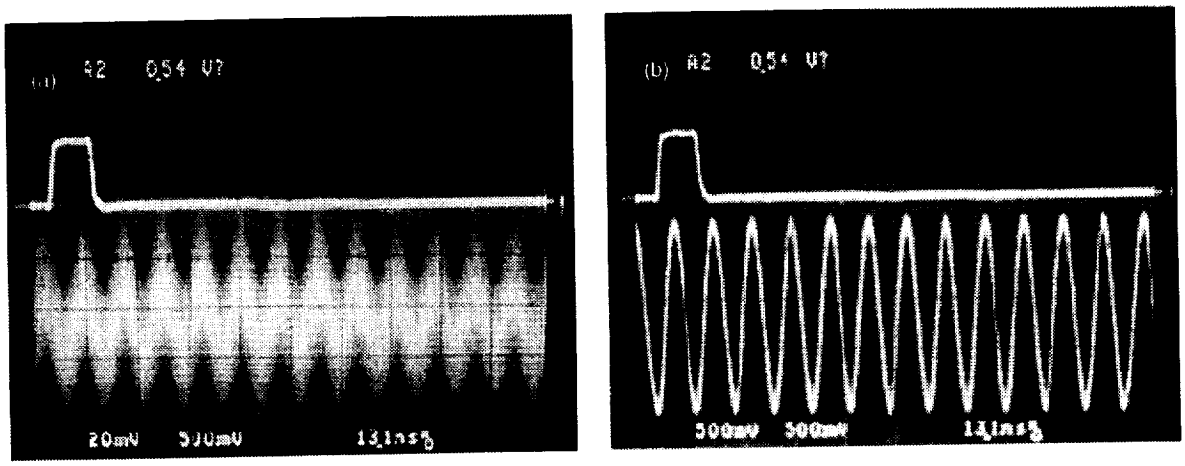

Fig. 9. Carrier recovery measurement in the time domain: (a) spoiled carrier and (b) recovered carrier.

The reason for choosing 100 MHz to demonstrate the clock and carrier recovery in the experiments above is because the measurement equipment we have (word generator, oscilloscope, and reference clock) operate around 100 MHz.

(2) The amplitude of the recovered signal (clock or carrier) is constant. It is independent of the input power of the signal to be recovered. This feature is especially important in clock recovery because the clock component contained in the received data stream varies with time and with sender (in a time division multiplexing system). The photonic clock regenerator ensures that the recovered clock has a constant power level at all times.

(3) The photonic clock and carrier regenerator can be accessed both optically and electronically. It has both electrical and optical inputs and outputs. This feature makes the device attractive in terms of easy interfacing with a complex fiber-optic communication system.

(4) Fast acquisition time for phase locking. Because the photonic clock and carrier regenerator is based on injection locking, its acquisition time is much faster than that of a clock recovery device based on a phase-locked loop [9]. Fast acquisition is important for high-speed telecommunications, especially for burst-mode communication. The estimated acquisition time is on the order of a microsecond or faster.

(5) Wide tracking range. The tracking range of the photonic clock and carrier regenerator is on the order of a few percent of the clock frequency, compared to a few tens of Hz for a clock recovery device based on a phase-locked loop. Having a wide tracking range makes the implementation of the device easier because the device does not have to be tuned precisely to match the incoming data rate.

(6) Frequency tunability. Unlike many other kinds of oscillators that can be tuned in only a narrow frequency band, the photonic oscillator can be tuned over many tens of MHz by changing the filter in the feedback loop and fine tuned by simply changing the loop delay or bias point of the E/O modulator. Delay line oscillators maintain high Q in spite of their ability to be tuned over a wide frequency range. This feature makes the device flexible in accommodating different systems, designs, and signal conditions.

(7) The device can be integrated on a chip. All of the key components of the device, such as the laser, the amplifier, the E/O modulator, and the photodetector can all be based on the GaAs technology and can be fabricated on the same substrate.

V. Applications

Figure 10 shows a clock recovery, synchronization, and signal recovery system based on the clock regenerator described here. An optical carrier containing high data-rate digital information arrives from a remote location and is split into two paths. One of these signals is injected into the photonic clock regenerator and the other signal is delayed in an optical delay line. The delay line is used to delay the received signal long enough for the clock regenerator to lock up so no data bits will be lost from the leading edge of the digital data stream. The recovered electrical clock is applied to the data recovery device in synchronization with the received signal, permitting the digital data to be recovered.

The recovered optical clock can be transmitted over optical fiber to be used by other devices within a several-kilometers area. This negates the need to have multiple clock recovery systems in a complex. Because of the high loss and dispersion of metallic transmission lines, it is not practical to use them to distribute a recovered 10-GHz clock over more than a few tens of meters.

In Fig. 11, the carrier regenerator is used as a clean-up loop for an analog frequency reference signal transmitted from a remote frequency reference. Again the regenerator has both an electrical and an optical output, so once the frequency reference is regenerated, it can be distributed locally over optical fiber.

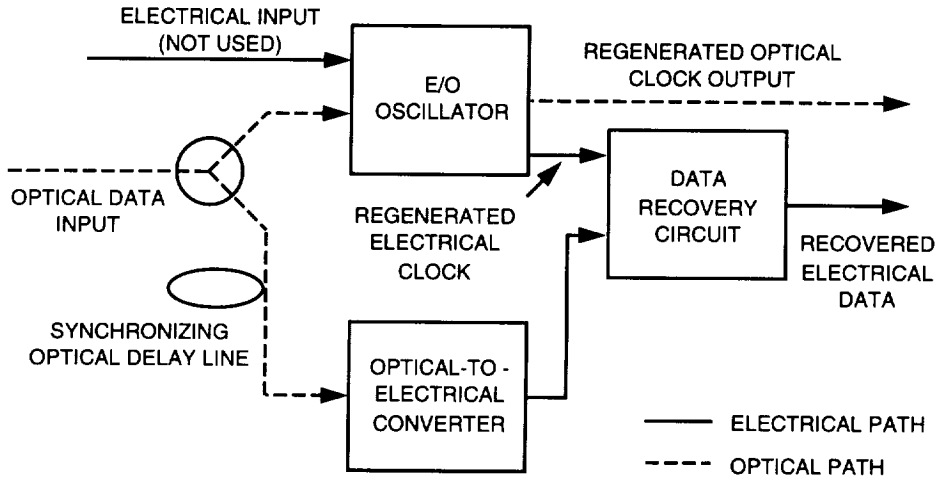

Fig. 10. Clock regenerator and data recovery system.

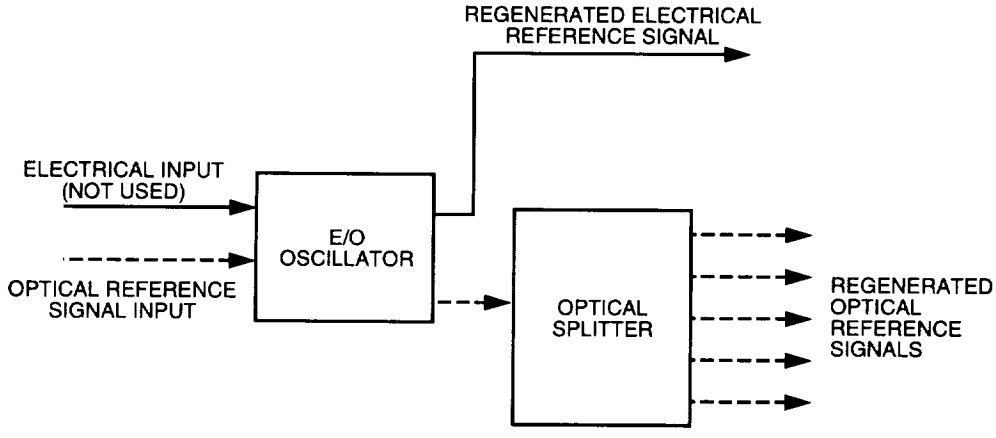

Fig. 11. Optical frequency reference regeneration and distribution.

References

[1] D. Wolever, *Phase-Locked Circuit Design*, Englewood Cliffs, New Jersey: Prentice Hall, 1991.

[2] K. Smith and J. K. Lucek, "All-Optical Clock Recovery Using a Mode-Locked Laser," *Electronic Letters*, vol. 28, no. 19, pp. 1814–1816, 1992.

[3] A. D. Ellis, K. Smith, and D. M. Patrick, "All Optical Clock Recovery at Bit Rates Up to 40 Gb/s," *Electronic Letters*, vol. 29, no. 15, pp. 1323–1324, 1993.

[4] D. M. Patrick and R. J. Manning, "20 Gb/s All-Optical Clock Recovery Using Semiconductor Nonlinearity," *Electronic Letters*, vol. 30, no. 2, pp. 15–152, 1994.

[5] P. E. Barnsley, H. J. Wicks, G. E. Wickens, and D. M. Spivit, "All-Optical Clock Recovery From 5 Gb/s RZ Data Using a Self-Pulsating 1.56 μm Laser Diode," *IEEE Photonics Technology Letters*, vol. 3, no. 10, pp. 942–945, 1991.

[6] M. Jinno and T. Matsumoto, "All-Optical Timing Extraction Using a 1.5 μm Self-Pulsating Multielectrode DFB LD," *Electronic Letters*, vol. 24, no. 23, pp. 1426–1427, 1988.

[7] X. S. Yao and L. Maleki, "High Frequency Optical Subcarrier Generator," *Electronic Letters*, vol. 30, no. 18, pp. 1525–1526, 1994.

[8] H. Ichino, M. Togashi, M. Ohhata, Y. Imai, N. Ishihata, and G. Sano, "Over 10 Gb/s ICs for Future Light Wave Communications," *J. Lightwave Technology*, vol. 12, no. 2, pp. 308–319, 1994.

[9] V. Vzunoglu and M. H. White, "The Synchronous Oscillator: A Synchronization and Tracking Network," *IEEE J. Solid State Circuits*, SC-2016, pp. 1214–1226, 1985.